Lasers Med Sci (2017) 32:663–672
DOI 10.1007/s10103-017-2165-2

ORIGINAL ARTICLE

Biochemical changes on the repair of surgical bone defects grafted with biphasic synthetic micro-granular HA + β-tricalcium phosphate induced by laser and LED phototherapies and assessed by Raman spectroscopy

Antônio Luiz Barbosa Pinheiro[1,2,3] · **Luiz Guilherme Pinheiro Soares**[1] · **Aparecida Maria Cordeiro Marques**[1,2] · **Maria Cristina Teixeira Cangussú**[1] · **Marcos Tadeu Tavares Pacheco**[3] · **Landulfo Silveira Jr.**[3]

Received: 14 September 2016 / Accepted: 31 January 2017 / Published online: 10 February 2017

Abstracts This work aimed the assessment of biochemical changes induced by laser or LED irradiation during mineralization of a bone defect in an animal model using a spectral model based on Raman spectroscopy. Six groups were studied: clot, laser ($\lambda = 780$ nm; 70 mW), LED ($\lambda = 850 \pm 10$ nm; 150 mW), biomaterial (biphasic synthetic micro-granular hydroxyapatite (HA) + β-tricalcium phosphate), biomaterial + laser, and biomaterial + LED. When indicated, defects were further irradiated at a 48-h interval during 2 weeks (20 J/cm^2 per session). At the 15th and 30th days, femurs were dissected and spectra of the defects were collected. Raman spectra were submitted to a model to estimate the relative amount of collagen, phosphate HA, and carbonate HA by using the spectra of pure collagen and biomaterials composed of phosphate and carbonate HA, respectively. The use of the biomaterial associated to phototherapy did not change the collagen formation at both 15 and 30 days. The amount of carbonate HA was not different in all groups at the 15th day. However, at the 30th day, there was a significant difference (ANOVA, $p = 0.01$), with lower carbonate HA for the group biomaterial + LED compared to biomaterial ($p < 0.05$). The phosphate HA was higher in the groups that received biomaterial grafts at the 15th day compared to clot (significant for the biomaterial; $p < 0.01$). At the 30th day, the phosphate HA was higher for the group biomaterial + laser, while this was lower for all the other groups. These results indicated that the use of laser phototherapy improved the repair of bone defects grafted with the biomaterial by increasing the deposition of phosphate HA.

Keywords Biomaterial · Bone repair · Laser and LED phototherapy · Biochemical assay · Raman spectroscopy

✉ Antônio Luiz Barbosa Pinheiro
albp@ufba.br

[1] Center of Biophotonics, School of Dentistry, Federal University of Bahia—UFBA, Av. Araújo Pinho, 62, Canela, Salvador, BA 40110-150, Brazil

[2] National Institute of Optics and Photonics, Physics Institute of São Carlos, University of São Paulo, São Carlos, SP 13560-970, Brazil

[3] Center for Innovation, Technology and Education—CITE, Universidade Anhembi Morumbi—UAM, Parque Tecnológico de São José dos Campos, Estr. Dr. Altino Bondensan, 500, Eugênio de Melo, São José dos Campos, SP 12247-016, Brazil

Introduction

Bone loss is a frequent challenge for surgeons as it may be caused by several etiologic factors [1] and the defects may be too large for spontaneous and physiologic repair. Autologous bone is the most common type of graft used to help the repair and it may be raised from several parts of the skeleton. Biocompatibility and osteointegration, as well as substantial osteogenic potential, characterize autologous bone grafts [2]. The use of autologous grafts remains the gold standard for the treatment of bone defects [3, 4].

Biomaterials have been proposed instead of using autologous grafts in order to minimize the morbidity of the procedures by avoiding two simultaneous surgical procedures. One of the most commonly used biomaterial in bone defects is the hydroxyapatite (HA). These biomaterials may be used isolated, associated with the use of membranes, or mixed to an autologous bone graft [4]. Both autologous and xenografts have been used to provide a framework or to stimulate new bone formation, and

studies showed that these grafts respond positively to the light irradiation of appropriate wavelength [1, 5].

The combination of HA + β-tricalcium phosphate (β-TCP) graft with phototherapy may have beneficial effects in bone repair because this biomaterial is considered a precursor of the HA and possesses osteoconductive properties. It is known that phototherapy influences function, proliferation, and secretion of growth factors such as bone morphogenetic proteins (BMPs), platelet-derived growth factor, and tumor growth factor β by different types of cells [4, 5]. This combination may modulate the repair of bone defects in a manner similar to what is observed following the use of autologous bone graft, preventing its limitations and complications [3–5]. As a means of improving the recovery of large bone defects, the use of techniques based on the use of grafts and photobioengineering has been extensively studied [4–10]. Recently, laser light has been used for improving bone repair in several conditions such as in autologous bone grafts [3, 4], dental implants [5], and several types of bone defects [6, 7, 10–12].

Several studies have demonstrated that the use of near-infrared phototherapy is mostly suitable for improving bone repair due to their higher penetration depth in the bone tissue when compared to visible light [4–8, 11–13]. Although the use of light phototherapy on bone repair has been growing steadily and that several studies have demonstrated positive results on the repair of bone tissue [4–8, 11–13], there are few reports on its association to biomaterials.

Light-emitting diode phototherapy (LED-PT) has been shown to induce a rapid repair process in bone defects using similar parameters to the ones carried out with laser phototherapy (L-PT). Studies demonstrated that the beneficial effects of LED-PT are likely similar to those of the L-PT [12, 13]. The mechanism involved might be similar to the light absorption by the mitochondrial membrane [14, 15], since the wavelength and fluence energy are more important than the type of equipment that generates the light. It has been demonstrated that light stimulates the cytochrome *C* oxidase from the mitochondria, causing increased energy production and stimulating mitochondrial oxidative metabolism [16]. Light may also modulate fibroblast proliferation, attachment, and synthesis of collagen and procollagen, promote angiogenesis, and stimulate macrophages and lymphocytes, thus accelerating bone repair process [1, 17].

Despite the growth of successful reports of phototherapies in hard tissues, their use in bone repair associated with grafting with biomaterials needs to be further studied as the constant development of new biomaterials that may induce different responses from the bone. Most biomaterials such as HA and similar ones demand longer time to be reabsorbed by the bone. As light has been proven to quickly repair bone, it would be desirable to develop a technique to ameliorate the time of bone repair in cases of the use of biomaterials. Our group has been studying the effects of the use of phototherapies on different models of bone repair by using Raman spectroscopy and the results of these studies showed that Raman spectroscopic techniques are effective on assessing the repair of bone defects [2, 7, 8, 10, 13, 18–21].

Raman spectroscopy has been used for the non-destructive biochemical analysis of biological samples, permitting a qualitative and quantitative evaluation of their biochemical composition and monitoring biological processes [22–25]. The Raman spectrum of bone shows prominent vibrational bands related to tissue composition: the Raman bands with peaks at ~960, ~1045, and ~1070 cm^{-1}, attributed to calcium HA (both carbonate and phosphate), and the bands with peaks at ~1450 and ~1660 cm^{-1}, attributed to collagen from the matrix [26]. Thus, Raman spectroscopy could be a method to assay bone mineralization and remodeling by evaluating the changes in the Raman bands, in situ and rapidly, without sample preparation or tissue destruction [26, 27].

As Raman bands could reveal the tissue constitution, researchers have proposed that the absolute or relative concentrations of most relevant biochemical and morphological structures present in a particular biological tissue could be estimated using the Raman spectra of such biochemical and morphological structures linearly fitted to the spectra of tissue samples [28–31], resulting in fitting coefficients directly related to the spectral contribution of these tissue components that would allow the evaluation of the absolute or relative concentrations of these compounds in each tissue type or group, and thus bringing diagnostic information. The application of such spectral model would reveal the biochemical alterations on bone constitution quantitatively due to the use of biomaterial graft followed by light irradiation.

The aim of this study was to evaluate the changes in the biochemistry of the induced repair process in bone defects filled with autologous blood clot or biomaterial (biphasic synthetic micro-granular HA + β-tricalcium phosphate) and associated or not with LED ($\lambda = 850 \pm 10$ nm) or laser ($\lambda = 780$ nm) phototherapy (20 J/cm^2 total energy) at 15 and 30 days after the beginning of defect treatment. A spectral model has been developed to estimate the relative concentration of the minerals (phosphate and carbonate) in the HA and organic matrix (collagen) related to the bone repair, using the spectra of pure collagen and biomaterials which are rich in phosphate and carbonate HA.

Materials and methods

Bone samples and phototherapy protocol

This study has been performed using the Raman spectra from bone samples collected in the previous works [8, 13, 19] and was approved by the Animal Ethics Committee of the School of Dentistry of the Federal University of Bahia (08/2010).

Briefly, 60 Wistar rats (male, ~2 months old, and average weight of 295 ± 25 g) were randomly distributed into six groups (clot, clot + LED, clot + laser, biomaterial, biomaterial + LED, and biomaterial + laser) and then subdivided into two subgroups according to the animal death time (15 and 30 days after the experimental procedure).

Animals were sedated (0.04 mL/100 g of atropine subcutaneously) and 20 min later, general anesthesia (10% ketamine − 0.1 mL/100 g of Cetamin®, Syntec, São Paulo, Brazil + 2% xylazin − 0.1 mL/100 g of Xilazin®, Syntec, São Paulo, Brazil) was carried out. The animals had their right leg shaved and a 3-cm-long incision was made at the right tibia with a no. 15 scalpel blade. Skin and subcutaneous tissues were dissected down to the periosteum, which was gently sectioned for exposing the bone, and a standard 2-mm round partial-thickness defect was surgically produced in each animal using low speed trephine drill (SIN, São Paulo, Brazil).

Defects on animals in groups clot, clot + LED, and clot + laser were filled with autologous blood clot. Defects on animals in groups biomaterial, biomaterial + LED, and biomaterial + laser were filled with the biomaterial biphasic synthetic micro-granular HA + β-tricalcium phosphate (70 and 30%, respectively; GenPhos®, Baumer, Mogi Mirim, SP, Brazil). The animals at the groups _+ LED and _+ laser were further irradiated with either laser or LED light as described below. All wounds were sutured and the animals received a single dose of antibiotics (Pentabiotico®, 0.2 mL, Fort Dodge Animal Health, Overland Park, KS, USA).

LED phototherapy was carried out using an LED device with wavelength of 850 ± 10 nm and power of 150 mW (model FisioLED®, MMOptics, São Carlos, São Paulo, Brazil; CW 128 s and irradiation area ~0.5 cm^2). Laser phototherapy was carried out using a diode laser with wavelength of 780 nm and power of 70 mW (model TwinFlex Evolution®, MMOptics, São Carlos, São Paulo, Brazil; CW 299 s and irradiation area ~0.04 cm^2). Energy fluence delivered for both devices was 20.4 J/cm^2. When the laser was used, it was transcutaneously applied in four points with 5.1 J/cm^2 each point around the defect at 48 h intervals during 2 weeks. When the LED was used, application was in a single point over the defect. The total energy density was 142.8 J/cm^2. Light was delivered in contact mode. The first session was carried out immediately after surgery. Energy densities used were based upon previous studies carried out by our group [2, 6, 10, 11].

Animal death occurred after 15 and 30 days after surgery in a CO_2 chamber (model EB 248, Insight Equipamentos, Ribeirão Preto, SP, Brazil), where the tibia with defect was removed with 5 mm margins. This block of tissue was longitudinally cut at the middle under refrigeration (driller 600 BML, SIN, São Paulo, SP, Brazil); one half was kept deep-refrigerated (−80 °C) for Raman spectral analysis and the other half was processed for histology.

Raman spectroscopy and spectral model

Raman spectra were collected using a dispersive near-infrared Raman spectrometer (785 nm laser excitation, 100 mW power output, imaging spectrograph with grating of spectral resolution of about 4 cm^{-1} in the spectral range from 700 to 1800 cm^{-1}, and back-illuminated, deep-depletion CCD camera) connected to a microcomputer. For the Raman scattering excitation and collection, the spectrometer is coupled to a fiber optic "Raman Probe" (model BAC-100-785, B&W TEK, Newark, DE, USA). The probe provides repeatable excitation–collection geometry. Spectrograph had the wavenumber and intensity calibration verified prior to the data collection.

Raman spectra were collected via the probe in five points at the defect with integration time set to 20 s. These spectra were pre-processed, first manually removing unwanted cosmic rays spikes in the output ASCII file and then removing the fluorescence background by fitting and subtracting a 5th order polynomial in the spectral range of 700–1800 cm^{-1}. The five spectra of each sample were averaged, resulting in 300 spectra that were used in the study.

A spectral model was developed by calculating the fitting coefficients (Raman estimators) of selected biocompounds that are expected to be present in bone tissue, using the unique biochemical information (fingerprint) provided by the spectra for each compound included in the model. Fitting of the spectra of bone constituents to the spectra of bone tissues was performed using ordinary least square analysis, according to the following expression [30]:

$$X = c \cdot S + E \quad (1)$$

where X is the original spectrum, S is the spectral matrix of selected tissue constituents, c is the matrix of their relative spectral contribution (fit parameter) predicted by the model, and E is the fitting residual. This expression can be used to provide a "best fit" of the spectral components or basis spectra found within the measured spectrum. The assumption is made that the spectral components selected are a linear superposition of the main components of the tissue spectra [28, 30] and the residual is minimized [30]. To obtain the predicted relative spectral contribution c of the biochemical in each tissue type, one can perform the following calculation using ordinary linear least squares fitting [32]:

$$c = X \backslash S \quad (2)$$

The Raman estimators c in Eq. (2) were calculated using Matlab® 6.0 (MathWorks, Natick, MA, USA) employing the linear least squares modeling function without constraint]($c = X \backslash S$, where the operator "\" is the Matlab command for matrix division that solves linear least squares models).

The model included primarily the biocompounds that presented Raman bands visually closer to the ones found in bone tissue. In this model, the biochemicals used are two biomaterials, Algipore® (Dentsply Ind. Com. Ltda., Petrópolis, RJ, Brazil) and Genphos® (Baumer, São Paulo, SP, Brazil), and collagen (ref. 9007-34-5, Sigma-Aldrich Brazil, São Paulo, SP, Brazil). The spectral feature of Algipore® was used to estimate the carbonate substitution in the HA lattice during the remodeling process, i.e., the maturation of the bone, and the biomaterial Genphos® was used to estimate the amount of biomaterial in the lesion site at the 15th day as well as the phosphate HA remnant from the bone remodeling process at the 30th day. The collagen is used to estimate the synthesis of bone matrix.

The Raman estimators were analyzed to verify their normality. The statistical analysis were applied in the Raman estimators employing the ANOVA between groups (followed by the Tukey post-test) and general linear model by comparing the differences regarding the light source, the type of treatment, and time, using Minitab 15.0® software (Minitab, Belo Horizonte, MG, Brazil). Differences between groups were considered significant when $p < 0.05$.

Results and discussion

Figure 1 shows the mean Raman spectrum of each group at the experimental times of 15 and 30 days. These spectra are dominated by bands of carbonate and phosphate HA and collagen [26, 27, 33–37]. During the repair process of bone, several biochemical changes occur. Differences in the peak intensity and position of specific bands indicate differences in the bone constitution and biochemical changes during remodeling induced by the therapy used. Particularly, the peak at ~961 cm^{-1}, attributed to ν_1 symmetric stretching of phosphate (PO_4^{3-}) of HA, and the peak at ~1071 cm^{-1}, attributed to ν_1 symmetric stretching of B-type carbonate (CO_3^{2-}) substitution in the HA lattice, showed differences in the peak intensity between the groups for both 15 and 30 days. Also, the peak at ~1047 cm^{-1}, attributed to ν_3 symmetric stretching vibration of phosphate (PO_4^{3-}) of HA, presented an increase in the intensity and shift in the position to higher wavenumber. The bands with peaks at ~1451 and ~1661 cm^{-1}, attributed to the CH_2/CH_3 bending/wagging of methylene side chain and C=O stretching vibration, α-helix conformation–amide I, respectively, from the collagen matrix, showed changes in the intensities between the groups. The contribution of each biochemical for these changes were modeled and presented.

In this work, the ability of the autologous blood clot versus the biomaterial irradiated or not with LED and laser light to stimulate bone mineralization and remodeling has been evaluated by using a spectral model based on the spectral features of the most common and relevant tissue scatterers. During the repair process of bone tissue, several biochemical changes occur on the composition of the bone. In order to estimate these changes, a spectral model has been applied to the spectra of all groups, with the aim to estimate the contribution of selected basal biochemical compounds, known to be presented during bone remodeling, to the observed spectra; therefore, these changes could be estimated quantitatively. Figure 2 shows the spectra of these biocompounds: the biomaterials Algipore® and Genphos®, and the collagen. In the spectral model, the spectral features presented in the Algipore® and Genphos® represent the carbonate and phosphate HA, respectively, particularly the strong peak at ~962 cm^{-1} that is shifted to lower wavenumber (~958 cm^{-1}) for carbonate HA, the peak at 1047 cm^{-1}, that presents lower intensity for the carbonate HA than the phosphate HA, and the one at 1071 cm^{-1}, that is lower intensity and shifted to higher wavenumber in the phosphate HA compared to the higher intensity of the carbonate HA. The Raman features of Genphos® represent a remodeled, end-stage mature bone, with about 10–15% of carbonate in the HA lattice, while the Algipore® represents the immature carbonate HA. Collagen features, particularly in the region of 1200–1800 cm^{-1}, are seen in the spectrum of Algipore® but are not present in the biomaterial Genphos®.

The proposed model estimates the relative concentration of each of these biocompounds in the bone tissue, by least squares fitting, assuming that these compounds are the most relevant scatters in bone tissue and the residual is minimized. Figure 3 presents the mean and standard deviation of the Raman estimators of each basal constituent in the spectra of bone of each group at the 15th and 30th days. Figure 4 presents the reconstructed spectra, where the respective Raman estimator multiplies the spectrum of each basal compound, and then these products are added to obtain the modeled spectrum. The compounds used in the spectral model gave a good fit and the residual along the spectrum is negligible.

In Fig. 3 (carbonate HA), there were no significant differences in the amount of carbonate HA versus clot ($p = 0.47$) at the 15th day, despite the (not significant) decrease of carbonate HA for the group biomaterial and increase for the clot + LED. At the 30th day, the carbonate HA of the group biomaterial + LED showed a significant decreased intensity compared to biomaterial ($p = 0.02$). This may suggest that the use of biomaterial alone is effective in producing carbonate HA, and the LED irradiation may inhibit the carbonate substitution at the 30th day of treatment. In Fig. 3 (phosphate HA), the group biomaterial presented higher phosphate HA versus clot ($p < 0.01$) at the 15th day, and all the groups biomaterial + LED and biomaterial + laser presented a (not significant) increase in the phosphate HA, certainly due to the presence of the biomaterial. At the 30th day, the higher phosphate HA was found in the group biomaterial + laser compared to clot ($p < 0.001$). This may suggest the presence of remnant phosphate HA in the groups containing biomaterial, principally the group biomaterial that was not

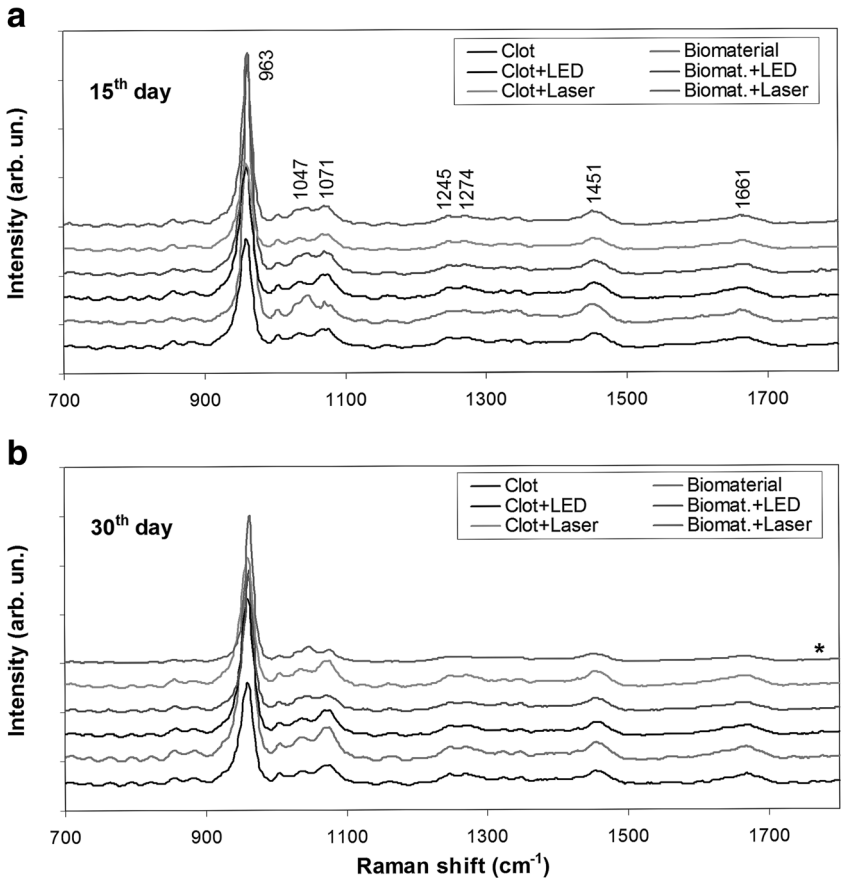

Fig. 1 Mean Raman spectra of all groups at the experimental times of **a** 15 and **b** 30 days. For scaling purposes, spectrum of biomaterial + laser at 30th day (*asterisk*) was divided by 3. Spectra were offset for better viewing. Excitation wavelength = 785 nm and spectral resolution = 4 cm^{-1}

osteointegrated during the remodeling process after 15 days, and also suggests an important bone remodeling and formation of phosphate HA after 30 days in the group biomaterial + laser. The Raman estimators for collagen indicated that for both 15 and 30 days, the use of biomaterial and irradiation with any of the light sources did not change the collagen synthesis at the lesion site ($p = 0.37$ and 0.18, respectively). Despite of not significant, the group biomaterial presented higher and the group biomaterial + LED presented lower amount of collagen for both 15 and 30 days. This may indicate that the biomaterial is inducing the formation of a new matrix and the LED irradiation may be inhibiting the matrix formation. This may be affecting the production of carbonate HA at the 30th day, as demonstrated by its lower amount in the group biomaterial + LED (Fig. 3, carbonate HA).

The results presented in this study is of importance in the study of the effect of filling agents such as autologous blood clot and β-TCP biomaterial in the new tissue formation after filling a bone defect. The reabsorption of the biomaterial at 15 days may be rapid in the group that received light therapy, more rapid for the laser group, as seen by the (not significant) decrease in the phosphate HA in these groups. On the other hand, after 30 days, these irradiated groups presented a higher phosphate HA content, significantly higher for the laser group. Interestingly, the biomaterial alone is capable of increasing the carbonate content in the HA of the filled defect after 30 days,

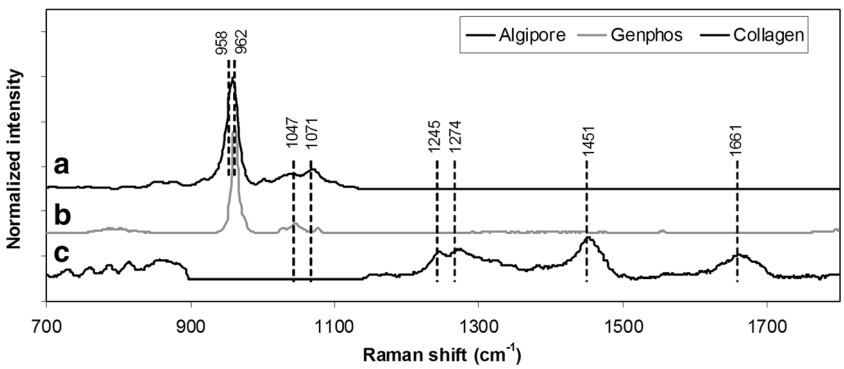

Fig. 2 Raman spectra of **a** biomaterial Algipore®, **b** biomaterial Genphos®, and **c** collagen. Spectra were offset for better viewing. In the spectra of Algipore® and collagen, the regions with common bands were cleared for better modeling. Excitation wavelength = 785 nm and spectral resolution = 4 cm^{-1}

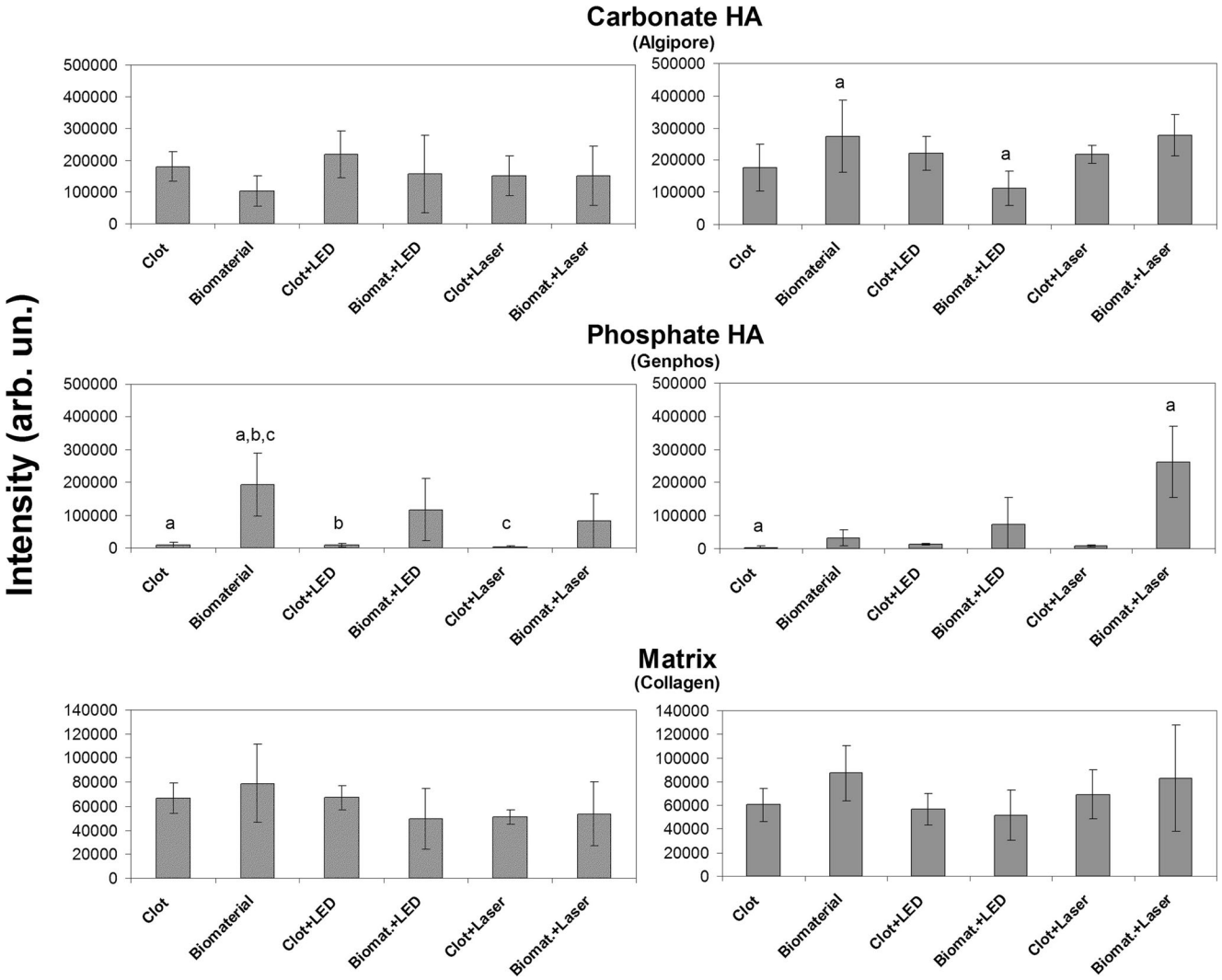

Fig. 3 Plot of the intensity of the Raman estimators of the compounds used in the spectral model (biomaterials Algipore® and Genphos®, and collagen) in each experimental group at 15th (*left*) and 30th day (*right*) after irradiation. *Superscript letters a*, *b*, and *c* indicates statistically significant differences between groups (ANOVA, the Tukey post-test, $p < 0.05$)

but LED irradiation may inhibit the carbonate substitution. On the other hand, the collagen content, that is an indicative of bone metabolism and remodeling, seems to be increased by the biomaterial and the laser irradiation. The not significant decrease in the collagen content at 15 and 30 days for the group biomaterial + LED may indicate inhibition of matrix production by the presence of the LED light.

Due to the complexity of the design of the study, ANOVA general linear model (GLM) was employed to verify if the variable use of phototherapy and/or time had influence on

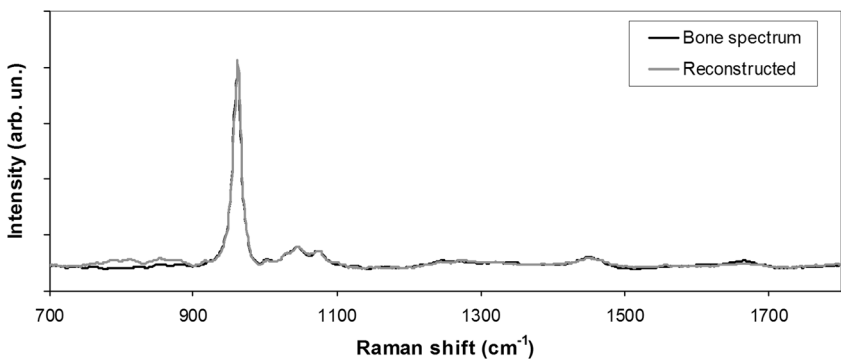

Fig. 4 Overlap of a sample spectrum of bone and the reconstructed spectrum, obtained by multiplying the spectrum of the basal compound with the respective Raman estimator, and adding the three compounds to form the modeled spectrum. A good fit was observed

the estimators of both the inorganic and organic components of the newly formed bone. A two-way ANOVA with balanced design was conducted. In this model, the differences in the biochemical composition of bone were evaluated depending on the predictor variables: type of treatment (clot, clot + LED, clot + laser, biomaterial, biomaterial + LED, and biomaterial + laser) and time (15 and 30 days), which were transformed into a "dummy variable." All the tests were conducted with a significance level of 5% ($p < 0.05$) and the adequacy of the models was evaluated with the adjusted R^2. A summary of the GLM analysis is seen on Table 1.

The ANOVA GLM indicated that the type of treatment influenced significantly the outcome of the carbonate HA ($p < 0.001$), which was also observed in the ANOVA (carbonate HA was significantly higher for the biomaterial at the 30th day; $p < 0.05$). The time of treatment was an important factor for significantly increasing the phosphate deposition ($p = 0.025$), also showed by ANOVA (higher phosphate HA for the groups that received biomaterial, $p < 0.05$), and consequent mineralization of the newly formed bone. This result suggests that the overall process, on regard the use or not of the biomaterial, differed between grafted and non-grafted defects, and is time-dependent. It is also possible to infer that the treatment influences the deposition of carbonated HA, which is a transitional HA, which will in a later stage lead to the transformation into phosphate HA during mineralization.

Figure 5 shows the correlation between the Raman estimators for collagen and carbonate HA contents for all the experimental groups at 15 and 30 days. It is interesting to observe a high correlation, which indicates that independently of the group, the collagen matrix synthesis is followed by the carbonate deposition in the collagen matrix. No correlation was found between the Raman estimators of collagen versus phosphate HA ($R^2 = 0.015$) and carbonate versus phosphate HA ($R^2 = 0.021$).

Bone mineralization is achieved by the local release of phosphate, which is generated by phosphatases present in osteoblast-derived, membrane-bound matrix vesicles within the osteoid. Together with the abundant calcium in the extracellular fluid, this results in nucleation and growth of crystals of hydroxyapatite [$Ca_{10}(PO4)_6(OH)_2$]. The proportion of organic matrix to mineral (in adult human cortical bone, approximately 60% mineral, 20% organic material, and 20% water) is crucial to ensure the correct balance between stiffness and flexibility of the skeleton. The carbonate content in the bone mineral is about 4–8 wt% and it depends on the age of the individual. Considering the hydroxyapatite structure, the carbonate group can substitute both the hydroxyl and the phosphate ions, giving rise to the A-type and B-type carbonation, respectively. The B-type is the preferential carbonate substitution found in the bone of a variety of species, with the A/B type ratio in the range 0.7–0.9. A higher value of the A/B ratio was observed in old tissue, compared to young tissue. The presence of B-carbonate in the apatite lattice was shown to cause a decrease in crystallinity and an increase in solubility in both in vitro and in vivo tests [38]. Moreover, the A-type HA surface showed a lower affinity for the human trabecular osteoblastic cell, compared to HA; this is demonstrated by the lower cell attachment and collagen production.

The assessment of bone mineralization induced by filling materials and light irradiation has been proposed in the literature, using the intensities of selected Raman peaks of carbonate and phosphate HA and collagen [2, 7, 8, 10, 13, 18], as well as ratios between the intensities of important Raman bands related to carbonate, phosphate, and collagen matrix [19]. The estimation of bone composition by a spectral model based on tissue biochemistry has not been proposed before.

Considering the Raman estimators of the biochemicals associated with mineralization and remodeling (biomaterials Algipore® and Genphos®–carbonate and phosphate HA, respectively, and collagen–bone matrix), it was evident that the use of phototherapy, particularly the laser, significantly affected the content of phosphate HA on biomaterial-filled defects. However, the fact that the biomaterial and LED also influenced the intensity of carbonate HA after 30 days is intriguing. One can speculate that the reason why the LED is not so efficient in promoting the maturity of the bone as laser does in the biomaterial-filled groups is probably related to the lower collagen

Table 1 Summary of the ANOVA general linear model for the Raman estimators of the biochemicals carbonate HA, phosphate HA, and collagen in the groups clot, clot + LED, clot + laser, biomaterial, biomaterial + LED, and biomaterial + laser, considering the variables: time (15th and 30th days) and treatment (clot, biomaterial, and laser)

Raman shifts	Association	Variable	Adjusted SS	*F*	*p* value
Carbonated HA (Algipore®)	Time × treatment	Time	1,182,029,944	0.19	0.664
		Treatment	40,966,144,440	6.64	<0.001*
Phosphate HA (Genphos®)	Time × treatment	Time	36,710,833,459	5.39	0.025*
		Treatment	9,411,366,745	1.38	0.248
Matrix (collagen)	Time × treatment	Time	608,056,222	1.08	0.303
		Treatment	1,108,166,365	1.97	0.100

*$p < 0.05$, statistically significant differences

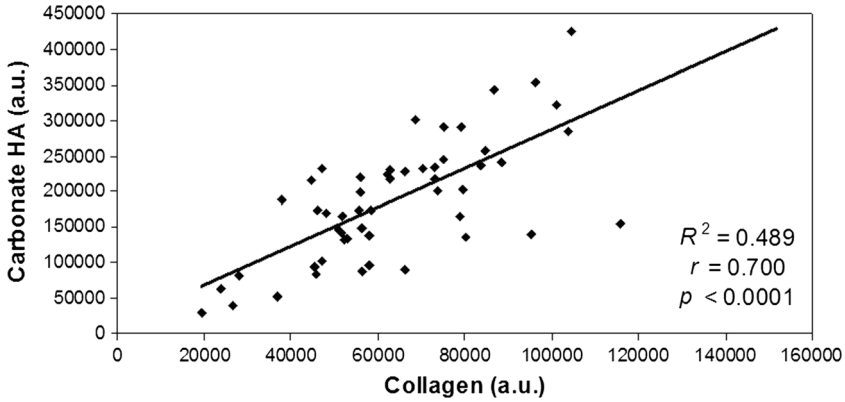

Fig. 5 Correlation between the Raman estimators of collagen versus carbonate HA in the groups at 15 and 30 days. The R^2, r, and p values are seen in the plot

formation induced by light irradiation, which occurs prior to the reabsorption and conversion of the biomaterial in phosphated bone. Then the time of 30 days may not be sufficient to have the complete carbonate substitution, necessary for the bone maturation. The presence of a phosphate HA-rich biomaterial induces the osteointegration process, and the results suggest that the use of laser light speeds this process of bone maturation. It is possible that the quick incorporation of the phosphate HA present on the biomaterial overlaps the carbonate substitution during mineralization. It is important to note that phosphate HA-based biomaterials and phosphated bone are indistinguishable from one another when using Raman spectroscopy.

Raman spectroscopy may provide an assessment of the reabsorption of the biomaterial by osteoclasts and the mineral synthesis by osteoblasts to make new bone, the so-called creeping substitution [39]. The findings may be indicative of an increased capacity of osteoclasts to break down the phosphate biomaterial and osteoblasts to secrete HA in irradiated bone tissue [4–6, 11, 12, 40], since during early stages of bone repair, the cellular component (chiefly fibroblasts and osteoblasts) is more prominent and more prone to be affected by the light. There is evidence that remodeling is taking place in the analysis of the Raman estimators of the phosphate HA at 15 and 30 days. Since the biomaterial is reabsorbed by the osteoclasts and the phosphated bone is formed by the osteoblasts, the Raman estimator for the phosphate HA decreased for the biomaterial-filled, non-irradiated group at 30 days compared to 15 days. As both irradiated groups have lower intensity compared to the biomaterial at the 15th day (not significant, $p > 0.05$), one can speculate that the light is accelerating the osteoclasts. As the laser-irradiated group presents higher intensity than the biomaterial at 30 days ($p < 0.0001$), one can state that the osteoblasts are producing phosphated bone.

The Raman estimators of phosphate HA may be used to estimate the concentration/incorporation of HA by the bone. The increase in bone HA is indicative of a more resistant bone as there is evidence that the degree of mineralization of bone tissue strongly influences the mechanical resistance of bones as well as the bone mineral density [41]. The results of this study indicate that the laser phototherapy has a potential to stimulate the osteointegration of the biomaterial by the increased deposition of phosphate HA throughout the repair time caused by irradiation with the laser and shows a progressive mineralization of the newly formed bone. This has been demonstrated in previous studies where biomaterial-grafted animals were irradiated with laser light and the intensity of the peak related to the phosphate at ~960 cm^{-1} continued to increase along the time [8, 13, 42]. However, the time interval of 30 days used in this work was not sufficient to evaluate an eventual increase in the carbonated HA. It is also important to note that the composition of the biomaterial used in the graft may influence the outcome of the repair, confirmed by previous studies using grafts containing BMPs [7, 43] and mineral trioxide aggregates (MTAs) [6, 9].

The overall results referred to inorganic and organic components during bone repair of defects filled with clot and biomaterial indicate that the type of light used affects significantly the outcome of the repair of such defects. From the results, it may be assumed that the association of the biomaterial with laser phototherapy achieved best results, corroborating previous reports [2, 7, 8, 10, 13].

The results when using phototherapies might be attributed to their effects on cellular reactions such as an increased ATP synthesis, stimulation of the electron transport chain, and pH reduction of the cells [16]. Other biochemical and conductivity of the cell membrane may also be affected by light and may result in an enhancement of the activity of macrophages, lymphocytes, and other cells involved in the repair. In addition, laser-irradiated tissues show both increased DNA synthesis and collagen deposition, increased deposition of Ca^+ [44], increased periosteal cell function [45], increased function of osteoblasts and osteocytes, and enhanced neovascularization

[1, 4–6, 11, 12]. All of these aspects have been previously reported as positive effects of the use of laser phototherapy on bone repair and explain the results of this study.

Conclusion

These results indicated that the use of laser phototherapy improved the repair of bone defects grafted with the biomaterial by increasing the deposition of phosphate HA as marked by biochemical estimators.

Acknowledgements The authors would like to thank the CNPq (Brazilian National Counsel of Technological and Scientific Development) and FAPESP (São Paulo Research Foundation—nos. 2009/01788-5 and 2015/24040-7) for the financial support that allowed this research.

Compliance with ethical standards

Conflict of interest The authors declare that there is no conflict of interest involving this paper.

References

1. Pinheiro ALB, Gerbi ME (2006) Photoengineering of bone repair processes. Photomed Laser Surg 24(2):169–178
2. Lopes CB, Pacheco MT, Silveira L, Duarte J, Cangussú MC, Pinheiro ALB (2007) The effect of the association of NIR laser therapy BMPs, and guided bone regeneration on tibial fractures treated with wire osteosynthesis: Raman spectroscopy study. J Photochem Photobiol B 89(3):125–130
3. Weber JBB, Pinheiro ALB, Oliveira MG, Oliveira FAM, Ramalho LMP (2006) Laser therapy improves healing of bone defects submitted to autogenous bone graft. Photomed Laser Surg 24(1):38–44
4. Torres CS, Santos JN, Monteiro JSC, Gomes PTCC, Pinheiro ALB (2008) Does the use of laser photobiomodulation, bone morphogenetic proteins, and guided bone regeneration improve the outcome of autologous bone grafts? An in vivo study in a rodent model. Photomed Laser Surg 26(4):371–377
5. Soares LGP, Magalhães EB, Magalhães CAB, Ferreira CF, Marques AMC, Pinheiro ALB (2013) New bone formation around implants inserted on autologous and xenografts irradiated or not with IR laser light: a histomorphometric study in rabbits. Braz Dent J 24(3):218–223
6. Pinheiro ALB, Soares LGP, Aciole GTS, Correia NA, Barbosa AF, Ramalho LMP, Santos JN (2011) Light microscopic description of the effects of laser phototherapy on bone defects grafted with mineral trioxide aggregate, bone morphogenetic proteins, and guided bone regeneration in a rodent model. J Biomed Mater Res A 98(2):212–221
7. Lopes CB, Pacheco MTT, Silveira L, Cangussu MCT, Pinheiro ALB (2010) The effect of the association of near infrared laser therapy, bone morphogenetic proteins, and guided bone regeneration on tibial fractures treated with internal rigid fixation: a Raman spectroscopic study. J Biomed Mater Res A 4(4):1257–1263
8. Soares LGP, Marques AMC, Barbosa AFS, Santos NR, Aciole JMS, Souza CMC, Pinheiro ALB, Silveira L (2014) Raman study of the repair of surgical bone defects grafted with biphasic synthetic microgranular HA + β-calcium triphosphate and irradiated or not with λ780 nm laser. Lasers Med Sci 29(5):1539–1550
9. Pinheiro ALB, Soares LGP, Barbosa AFS, Ramalho LMP, Santos JN (2012) Does LED phototherapy influence the repair of bone defects grafted with MTA, bone morphogenetic proteins, and guided bone regeneration? A description of the repair process on rodents. Lasers Med Sci 27(5):1013–1024
10. Pinheiro ALB, Santos NR, Oliveira PC, Aciole GT, Ramos TA, Gonzalez TA, Silva LN, Barbosa AF, Silveira L (2013) The efficacy of the use of IR laser phototherapy associated to biphasic ceramic graft and guided bone regeneration on surgical fractures treated with miniplates: a Raman spectral study on rabbits. Lasers Med Sci 28(2):513–518
11. Pinheiro ALB, Gerbi MEMM, Limeira Junior FA, Ponzi EAC, Marques AMC, Carvalho CM, Santos RC, Oliveira PC, Nóia M, Ramalho LMP (2009) Bone repair following bone grafting hydroxyapatite guided bone regeneration and infrared laser photobiomodulation: a histological study in a rodent model. Lasers Med Sci 24(2):234–240
12. Soares LG, Marques AM, Guarda MG, Aciole JM, Pinheiro AL, dos Santos JN (2015) Repair of surgical bone defects grafted with hydroxylapatite + β-TCP and irradiated with λ=850 nm LED light. Braz Dent J 26(1):19–25
13. Pinheiro ALB, Soares LGP, Cangussú MCT, Santos NR, Barbosa AFS, Silveira L (2012) Effects of LED phototherapy on bone defects grafted with MTA, bone morphogenetic proteins and guided bone regeneration: a Raman spectroscopic study. Lasers Med Sci 27(5):903–916
14. Al-Watban FA, Andres BL (2006) Polychromatic LED in oval full-thickness wound healing in non-diabetic and diabetic rats. Photomed Laser Surg 24(1):10–16
15. Weiss RA, Mcdaniel DH, Geronemus RG, Weiss MA, Beasley KL, Munavalli GM, Bellew G (2005) Clinical experience with light emitting diode (LED) photomodulation. Dermatol Surg 31(9):1199–1205
16. Karu TI, Pyatibrat LV, Afanasyeva NI (2004) A novel mitochondrial signaling pathway activated by visible-to-near infrared radiation. Photochem Photobiol 80(2):366–372
17. Pinheiro ALB, Oliveira MG, Martins PPM, Ramalho LMP, Oliveira MAM, Novaes A, Nicolau RA (2001) Biomodulatory effects of LLLT on bone regeneration. Lasers Ther 13:73–79
18. Soares LG, Marques AM, Guarda MG, Aciole JM, Andrade AS, Pinheiro AL, Silveira L (2014) Raman spectroscopic study of the repair of surgical bone defects grafted or not with biphasic synthetic micro-granular HA + β-calcium triphosphate irradiated or not with λ850 nm LED light. Lasers Med Sci 29(6):1927–1936
19. Pinheiro AL, Soares LG, Marques AM, Aciole JM, de Souza RA, Silveira L (2014) Raman ratios on the repair of grafted surgical bone defects irradiated or not with laser (λ780 nm) or LED (λ850 nm). J Photochem Photobiol B 138:146–154
20. de Castro IC, Rosa CB, Dos Reis Júnior JA, Moreira LG, Aragão JS, Barbosa AF, Silveira L, Pinheiro AL (2014) Assessment of the use of LED phototherapy on bone defects grafted with hydroxyapatite on rats with iron-deficiency anemia and nonanemic: a Raman spectroscopy analysis. Lasers Med Sci 29(5):1607–1615
21. Aciole JM, de Castro IC, Soares LG, Barbosa AF, Aciole GT, Silveira L, Pinheiro ALB (2014) Assessment of the LED phototherapy on femoral bone defects of ovariectomized rats: a Raman spectral study. Lasers Med Sci 29(3):1269–1277
22. Hanlon B, Manoharan R, Koo TW, Shafer KE, Motz JT, Fitzmaurice M, Kramer JR, Itzkan I, Dasari RR, Feld MS (2000) Prospects for in vivo Raman spectroscopy. Phys Med Biol 45(2):R1–R59
23. Moreira LM, Silveira L, Santos FV, Lyon JP, Rocha R, Zângaro RA, Villaverde AB, Pacheco MTT (2008) Raman spectroscopy: a powerful technique for biochemical analysis and diagnosis. Spectrosc Int J 22:1–19
24. Krafft EC, Dietzek B, Schmitt M, Popp J (2012) Raman and coherent anti-Stokes Raman scattering microspectroscopy for biomedical applications. J Biomed Opt 17(4):040801

25. Pence I, Mahadevan-Jansen A (2016) Clinical instrumentation and applications of Raman spectroscopy. Chem Soc Rev 45(7):1958–1979
26. Morris MD, Mandair GS (2011) Raman assessment of bone quality. Clin Orthop Relat Res 469(8):2160–2169
27. Carden A, Morris MD (2000) Application of vibrational spectroscopy to the study of mineralized tissues (review). J Biomed Opt 5(3):259–268
28. Brennan JF III, Römer TJ, Lees RS, Tercyak AM, Kramer JR, Feld MS (1997) Determination of human coronary artery composition by Raman spectroscopy. Circulation 96(1):99–105
29. Haka AS, Volynskaya Z, Gardecki JA, Nazemi J, Lyons J, Hicks D, Fitzmaurice M, Dasari RR, Crowe JP, Feld MS (2006) In vivo margin assessment during partial mastectomy breast surgery using Raman spectroscopy. Cancer Res 66(6):3317–3322
30. Stone N, Prieto MCH, Crow P, Uff J, Ritchie AW (2007) The use of Raman spectroscopy to provide an estimation of the gross biochemistry associated with urological pathologies. Anal Bioanal Chem 387(5):1657–1668
31. Silveira L, Silveira FL, Bodanese B, Zângaro RA, Pacheco MTT (2012) Discriminating model for diagnosis of basal cell carcinoma and melanoma in vitro based on the Raman spectra of selected biochemicals. J Biomed Opt 17(7):077003
32. Moler C (2008) Least squares. In: Moler C (ed) Numerical computing with MATLAB: electronic edition. The MathWorks Inc., Natick, http://www.mathworks.com/moler/leastsquares.pdf. Accessed 20 May 2014
33. Penel G, Leroy G, Rey C, Bres E (1998) MicroRaman spectral study of the PO4 and CO3 vibrational modes in synthetic and biological apatites. Calcif Tissue Int 63(6):475–481
34. Timlin JA, Carden A, Morris MD (1999) Chemical microstructure of cortical bone probed by Raman transects. Appl Spectrosc 53(11): 1429–1435
35. Penel G, Cau E, Delfosse C, Rey C, Hardouin JJ, Delecourt C, Lemaitre J, Leroy G (2003) Raman microspectrometry studies of calcified tissues and related biomaterials. Raman studies of calcium phosphate biomaterials. Dent Med Probl 40(1):37–43
36. Okagbare PI, Begun D, Tecklenburg M, Awonusi A, Goldstein SA, Morris MD (2012) Noninvasive Raman spectroscopy of rat tibiae: approach to in vivo assessment of bone quality. J Biomed Opt 17(9):90502-1
37. Movasaghi Z, Rehman S, Rehman IU (2007) Raman spectroscopy of biological tissues. Appl Spectrosc Rev 42(5):493–541
38. Le Geros RZ (1991) Calcium phosphates in oral biology and medicine. In: Karger MH (ed) Monographs in oral science. AG Publishers, Basel, pp 82–107
39. Bauer TW, Muschler GF (2000) Bone graft materials: an overview of the basic science. Clin Orthop Relat Res 371:10–27
40. Kalfas H (2001) Principles of bone healing. Neurosurg Focus 10(4): 1–4
41. Boivin G, Meunier PJ (2003) The mineralization of bone tissue: a forgotten dimension in osteoporosis research. Osteoporos Int 14(Suppl 3):S19–S24
42. Carvalho FB, Aciole GTS, Aciole JMS, Silveira L, Santos JN, Pinheiro ALB (2011) Assessment of bone healing on tibial fractures treated with wire osteosynthesis associated or not with infrared laser light and biphasic ceramic bone graft (HATCP) and guided bone regeneration (GBR): Raman spectroscopic study. Proc. SPIE 7887: 7887OT-1
43. Pinheiro ALB, Gerbi MEM, Ponzi EAC, Ramalho LMP, Marques AMC, Carvalho CM, Santos RC, Oliveira PC, Nóia M (2008) Infrared laser light further improves bone healing when associated with bone morphogenetic proteins and guided bone regeneration: an in vivo study in a rodent model. Photomed Laser Surg 26(2): 167–174
44. Yamada K (1991) Biological effects of low power Laser irradiation on clonal osteoblastic cells (MC3T3-E1). J Jpn Orthop Assoc 65(9): 101–114
45. Trelles MA, Mayayo E (1987) Bone fracture consolidate faster with low power laser. Lasers Surg Med 7(1):36–45